

Supporting Information

Structural Evolution that Affects the Room-Temperature Internal Friction of Binary Oxide Nanolaminates: Implications for Ultrastable Optical Cavities

Le Yang,^{*a} Mariana Fazio,^b and Gabriele Vajente,^c Alena Ananyeva,^c GariLynn Billingsley,^d Ashot Markosyan,^d Riccardo Bassiri,^d Martin M. Fejer,^d Carmen S. Menoni^{b†}

^a Department of Chemistry, Colorado State University, Fort Collins, CO 80523, USA; E-mail: yangle@colostate.edu

^b Department of Electrical and Computer Engineering, Colorado State University, Fort Collins, CO 80523, USA

^c LIGO Laboratory, California Institute of Technology, Pasadena, CA 91125, USA

^d Edward L. Ginzton Laboratory, Stanford University, Stanford, CA 94305, USA

*corresponding author

Sample Preparation

Thin film samples in this work were prepared with a 4WAVE LANS® biased target reactive ion beam sputtering deposition system. A negative bias is applied to the metal targets with a positive pulse width. The pulse width/pulse period indicates the time when the target is not biased. For the growth of nanolaminates one metal target was biased sequentially while the other one was protected with a shutter. The mixtures were deposited with both targets being biased simultaneously. Different pulse widths were applied to each target to vary the cation concentration. Detailed deposition conditions for each sample are shown in Table S1 and S2.

Table S1. Deposition conditions of the nanolaminates.

nanolaminate		Target Bias (V)	Discharge Voltage (V)	Discharge Current (A)	Oxygen flow (sccm)	Pulse width /Pulse period
TiO ₂ /Ta ₂ O ₅	TiO ₂	800	50	5.7	3	62/100
	Ta ₂ O ₅	800	50	5.7	3	62/100
SiO ₂ /Ta ₂ O ₅	SiO ₂	800	50	5.7	3	75/100
	Ta ₂ O ₅	800	50	5.7	3	62/100

Table S2. Deposition conditions of the mixtures.

mixture		Target Bias (V)	Discharge Voltage (V)	Discharge Current (A)	Oxygen flow (sccm)	Pulse width /Pulse period
TiO ₂ /Ta ₂ O ₅	TiO ₂	800	50	5.7	4	2/100
	Ta ₂ O ₅					53/100
SiO ₂ /Ta ₂ O ₅	SiO ₂	800	50	5.7	12	92/100
	Ta ₂ O ₅					64/100

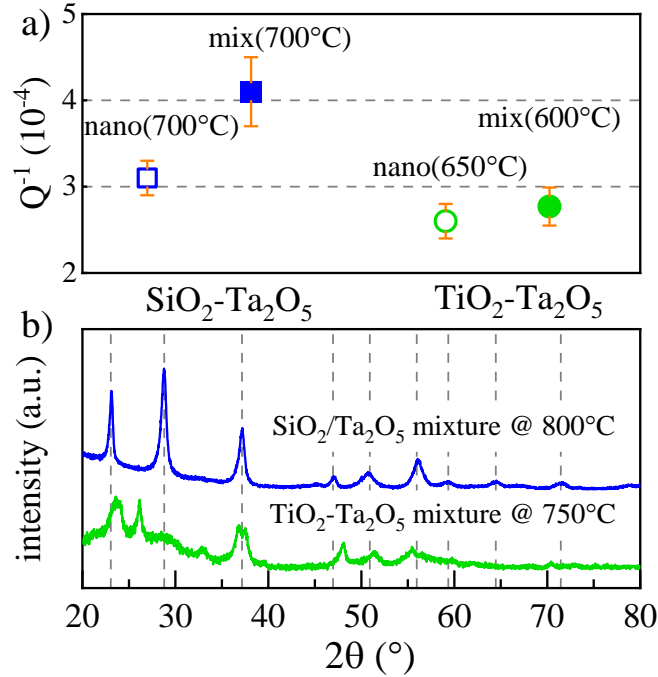


Fig. S1. a) Comparison of the internal friction of the nanolaminates and mixtures. For $\text{SiO}_2/\text{Ta}_2\text{O}_5$, the mixture has a higher internal friction than the nanolaminate, while for $\text{TiO}_2/\text{Ta}_2\text{O}_5$, the internal friction of the nanolaminate and mixture are the same within experimental error. b) Diffraction spectra of crystallized $\text{SiO}_2/\text{Ta}_2\text{O}_5$ and $\text{TiO}_2/\text{Ta}_2\text{O}_5$ mixtures after annealing. Phase separation in the annealed $\text{SiO}_2/\text{Ta}_2\text{O}_5$ mixture is identified with the crystallized phase being orthorhombic Ta_2O_5 . The mixture consists of a dominant Ta_2O_5 matrix with dispersed SiO_2 polyhedra. It behaves similarly to a single layer Ta_2O_5 . A ternary phase of $\text{TiTa}_{18}\text{O}_{47}$ is identified in the $\text{TiO}_2/\text{Ta}_2\text{O}_5$ mixture after annealing.

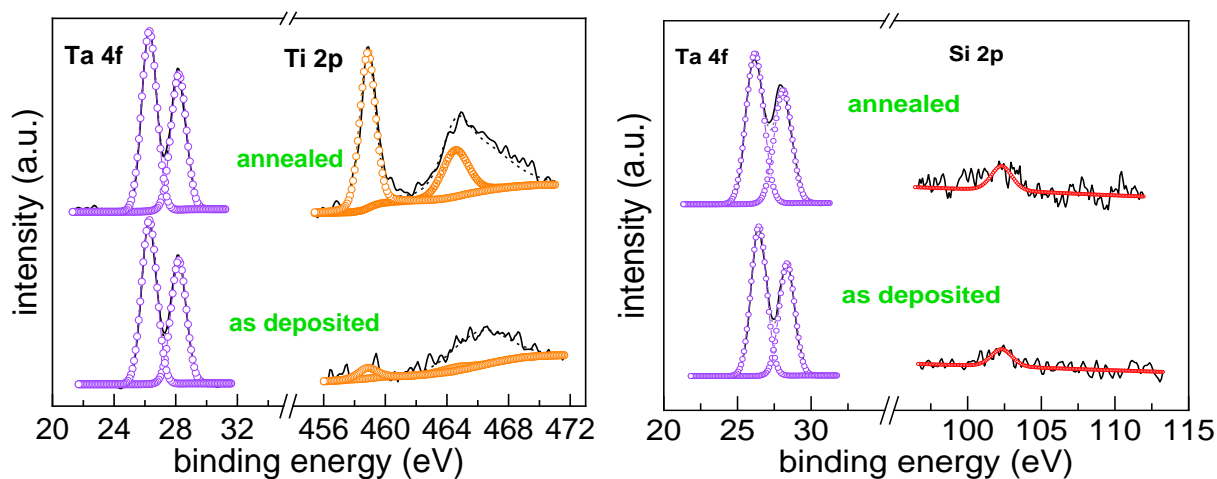


Fig. S2. Left, Ta 4f and Ti 2p peaks for the $\text{TiO}_2/\text{Ta}_2\text{O}_5$ nanolaminate as deposited and after annealing at 650°C . The emergence of Ti 2p peaks after annealing indicates a significant Ti cation diffusion into the top Ta_2O_5 layer. Right, Ta 4f and Si 2p peaks for the $\text{SiO}_2/\text{Ta}_2\text{O}_5$ nanolaminate as deposited and after annealing at 650°C . A negligible amount of Si is present in the top Ta_2O_5 layer before and after annealing. The peak area ratio between the Ta 4f and Si 2p peaks remains constant for as deposited and annealed samples. Si cation diffusion into the Ta_2O_5 layer upon annealing is not identified.